

# Characterization of hydromedusan $\text{Ca}^{2+}$ -regulated photoproteins as a tool for measurement of $\text{Ca}^{2+}$ concentration

Natalia P. Malikova · Ludmila P. Burakova ·  
Svetlana V. Markova · Eugene S. Vysotski

Received: 16 February 2014 / Revised: 30 May 2014 / Accepted: 18 June 2014 / Published online: 11 July 2014  
© Springer-Verlag Berlin Heidelberg 2014

**Abstract** Calcium ion is a ubiquitous intracellular messenger, performing this function in many eukaryotic cells. To understand calcium regulation mechanisms and how disturbances of these mechanisms are associated with disease states, it is necessary to measure calcium inside cells.  $\text{Ca}^{2+}$ -regulated photoproteins have been successfully used for this purpose for many years. Here we report the results of comparative studies on the properties of recombinant aequorin from *Aequorea victoria*, recombinant obelins from *Obelia geniculata* and *Obelia longissima*, recombinant mitrocomin from *Mitrocoma cellularia*, and recombinant clytin from *Clytia gregaria* as intracellular calcium indicators in a set of identical in vitro and in vivo experiments. Although photoproteins reveal a high degree of identity of amino acid sequences and spatial structures, and, apparently, have a common mechanism for the bioluminescence reaction, they were found to differ in the  $\text{Ca}^{2+}$  concentration detection limit, the sensitivity of bioluminescence to  $\text{Mg}^{2+}$ , and the rates of the rise of the luminescence signal with a sudden change of  $\text{Ca}^{2+}$

concentration. In addition, the bioluminescence activities of Chinese hamster ovary cells expressing wild-type photoproteins also differed. The light signals of cells expressing mitrocomin, for example, slightly exceeded the background, suggesting that mitrocomin may be hardly used to detect intracellular  $\text{Ca}^{2+}$  without modifications improving its properties. On the basis of experiments on the activation of endogenous  $\text{P2Y}_2$  receptor in Chinese hamster ovary cells by ATP, we suggest that wild-type aequorin and obelin from *O. longissima* are more suitable for calcium detection in cytoplasm, whereas clytin and obelin from *O. geniculata* can be used for calcium measurement in cell compartments with high  $\text{Ca}^{2+}$  concentration.

**Keywords** Calcium · Coelenterazine · Aequorin · Obelin · Clytin · Mitrocomin

Published in the topical collection *Analytical Bioluminescence and Chemiluminescence* with guest editors Elisa Michelini and Mara Mirasoli.

**Electronic supplementary material** The online version of this article (doi:10.1007/s00216-014-7986-2) contains supplementary material, which is available to authorized users.

N. P. Malikova · L. P. Burakova · S. V. Markova · E. S. Vysotski (✉)  
Photobiology Laboratory, Institute of Biophysics, Russian Academy  
of Sciences, Siberian Branch, Krasnoyarsk 660036, Russia  
e-mail: eugene.vysotski@gmail.com

E. S. Vysotski  
e-mail: eugene\_vysotski@ibp.ru

N. P. Malikova · L. P. Burakova · S. V. Markova · E. S. Vysotski  
Laboratory of Bioluminescent Biotechnologies, Institute of  
Fundamental Biology and Biotechnology, Siberian Federal  
University, Krasnoyarsk 660041, Russia

## Introduction

The  $\text{Ca}^{2+}$ -regulated photoproteins are “precharged” bioluminescent proteins that are triggered to emit light by binding calcium or certain other inorganic ions [1]. The reaction does not require the presence of molecular oxygen or any other cofactor—the photoprotein and the triggering ion are the only components required for light emission. Since the energy emitted as light is derived from the “charged” photoprotein, the molecule can react only once, i.e., it does not “turn over” as an enzyme does. In this respect, as well as in the lack of a requirement for molecular oxygen or any other cofactor, the reaction strikingly differs from that of classic bioluminescent systems in which an enzyme (luciferase) catalyzes the oxidation of a smaller organic substrate molecule (luciferin) yielding an excited state and light emission. This feature prompted Shimomura and Johnson [2] to coin the term “photoprotein”

to describe proteins that serve as the sole organic molecular species in bioluminescent reaction systems.

Although other kinds of photoproteins (photoprotein from the marine worm *Chaetopterus variopedatus* [3], pholasin from the marine bivalve *Pholas dactylus* [4, 5], and symplectin from the luminous squid *Symplectoteuthis oualaniensis* [6]) have been described, the great majority of photoproteins presently known are stimulated to luminesce by calcium [1, 7]. The best known and best studied of these are aequorin, first isolated in 1962 by Shimomura et al. [8] from the jellyfish *Aequorea victoria*, and obelin from the hydroid *Obelia longissima* [9]. All  $\text{Ca}^{2+}$ -regulated photoproteins isolated to date consist of a single-chain polypeptide to which an oxygen-activated substrate, 2-hydroperoxycoelenterazine, is tightly but noncovalently bound [10]. The existence of the bound peroxy-substituted coelenterazine was directly confirmed by determination of spatial structures of hydromedusan photoproteins from different organisms [11–13]. The bioluminescence reaction is an oxidative decarboxylation of 2-hydroperoxycoelenterazine with the elimination of 1 mol of carbon dioxide and generation of the protein-bound product (called coelenteramide) in the  $S_1$  excited state [14, 15]. The excited coelenteramide then relaxes to its ground state with the production of blue light of a broad spectrum with a maximum within the range 465–495 nm, depending on the photoprotein type [16].

Although  $\text{Ca}^{2+}$ -regulated photoproteins have apparently been detected in a variety of marine organisms [7], cloning and sequence analysis have been achieved for only five hydromedusan photoproteins—aequorin from *A. victoria* [17–19], clytin (also known as phialidin) from *Clytia gregaria* [20–22], mitrocomin (also known as halistaurin) from *Mitrocoma cellularia* [23], and obelins from *O. longissima* [24, 25] and *Obelia geniculata* [26]—and for light-sensitive photoproteins from the ctenophores *Beroë abyssicola* [27], *Mnemiopsis leidyi* [28, 29], and *Bathocyroe fosteri* [30]. Although hydromedusan and ctenophore photoproteins are functionally identical in many properties, contain three  $\text{Ca}^{2+}$ -binding sites characteristic of the EF-hand  $\text{Ca}^{2+}$ -binding proteins, and retain the same spatial architecture [31], the degree of identity of their amino acid sequences is only approximately 29 % [27, 30]. Apophotoproteins can be converted into active photoproteins by incubating them with coelenterazine under calcium-free conditions in the presence of  $\text{O}_2$  and reducing agents [32].

$\text{Ca}^{2+}$ -regulated photoproteins have attracted great interest owing to their broad analytical potential. The main application of photoproteins derives from their ability to emit light on  $\text{Ca}^{2+}$  binding, allowing them to be used to detect calcium ions in biological systems. It has been more than four decades since the  $\text{Ca}^{2+}$ -regulated photoprotein aequorin was first used as an intracellular  $\text{Ca}^{2+}$  indicator [33]. Although  $\text{Ca}^{2+}$ -regulated photoproteins, mostly aequorin, are still the indicators of

choice for some applications, they have now been largely eclipsed by the fluorescent tetracarboxylate calcium indicators introduced by Tsien [34]. These substances rapidly gained popularity because of their ready availability, stability, and ease of introduction into cells [35]. As experience with these indicators has grown, it has become increasingly clear that they have problems of their own, some of which are subtle but nonetheless serious [36–38]. The cloning of complementary DNAs encoding apophotoproteins has opened new avenues for utilizing photoproteins, by expressing the recombinant apophotoprotein intracellularly, then adding coelenterazine externally, which then diffuses into the cell and forms an active photoprotein. Such cells have, in effect, a “built-in” calcium indicator. This approach to measure intracellular  $\text{Ca}^{2+}$  concentration is highly effective and has many advantages over fluorescent  $\text{Ca}^{2+}$  probes: because it is a protein, photoprotein can be engineered to induce specific targeting sequences, permitting selective localization of the photoprotein to a cell region of interest; the background in photoprotein measurements is very low, resulting in a high signal-to-noise ratio, wide dynamic range, and low  $\text{Ca}^{2+}$ -buffering effect [38, 39]. The major disadvantage of photoproteins is the low light signals from cells because the photoprotein does not “turn over” as an enzyme does, and because only a small fraction of the photoprotein pool emits light throughout the experiment. This is not a problem when recordings from a microplate well with cells expressing photoprotein are performed. However, it is often desirable to measure  $\text{Ca}^{2+}$  concentration in a single cell. Although single-cell imaging experiments with recombinant aequorin have been performed [40, 41], they are technically difficult since these experiments require special imaging systems. In addition, since photoprotein may be distributed between cell regions with high and low  $\text{Ca}^{2+}$  concentration, the average rise in  $\text{Ca}^{2+}$  concentration may be overestimated because of a much larger photoprotein discharging in the region with high  $\text{Ca}^{2+}$  concentration [38, 39]. Wild-type aequorin, for example, is well suited to measure  $\text{Ca}^{2+}$  concentration between approximately 0.5 and 10  $\mu\text{M}$  [39]. However this dynamic range is insufficient when the photoprotein is targeted to intracellular compartments with high  $\text{Ca}^{2+}$  concentration. This drawback of aequorin had been overcome either through amino acid mutations in  $\text{Ca}^{2+}$ -binding loops and their adjacent  $\alpha$ -helices, leading to reduced photoprotein affinity for calcium [42–44], or by the use of synthetic coelenterazine analogues [45, 46]. Combination of these approaches decreases photoprotein affinity even more, allowing  $\text{Ca}^{2+}$  concentration measurement in mitochondria, endoplasmic reticulum, and Golgi apparatus [44, 47]. In the past decade, a new generation of genetically encoded calcium indicators based on green fluorescent protein have been developed. The best known of these are cameleons, camgaros, and pericams [37]. Although they have some advantages over chemical fluorescent probes (no dependence

of sensitivity and  $\text{Ca}^{2+}$ -binding kinetics on indicator concentration, precise expression in targeted intracellular compartments) and photoproteins (ratiometric  $\text{Ca}^{2+}$  concentration measurements, reversible  $\text{Ca}^{2+}$ -dependent fluorescent response, no need for specific cofactors, relatively bright fluorescence, and comparatively high temporal resolution), these  $\text{Ca}^{2+}$  indicators based on green fluorescent protein also have some drawbacks: small dynamic range of fluorescence intensity as compared with that of fluorescent dyes and sensitivity of fluorescence to pH [37, 48]. Thus, all  $\text{Ca}^{2+}$  indicators have both advantages and shortcomings, and the choice of which one to use depends on the biological task to be addressed.

Despite the availability of other recombinant photoproteins, only aequorin is widely used as an intracellular  $\text{Ca}^{2+}$  indicator, perhaps because it was the first to be discovered and well characterized. However, it has a number of drawbacks that limit its utility. The most significant shortcomings are that aequorin responds too slowly to faithfully follow the rapid intracellular calcium transients of nerves and some kinds of muscle, and that physiological concentrations of free magnesium [49, 50] antagonize the effects of calcium and slow the kinetics even further [51, 52]. The photoproteins of other coelenterates do not potentially share these defects in equal measure. It is well known, for example, that obelins from *O. longissima* and *O. geniculata* respond considerably faster on a sudden change of  $\text{Ca}^{2+}$  concentration and are relatively insensitive to magnesium concentration [26, 53, 54]. Besides, clytin and mitrocomin are reportedly less sensitive to calcium [55], and thus these photoproteins may be suitable for calcium measurements in cell organelles with high  $\text{Ca}^{2+}$  concentration without photoprotein modification. Although some photoproteins were characterized in terms of their applicability as calcium probes, this information is frequently incomplete and fragmentary.

In this study, we characterize five recombinant hydromedusan  $\text{Ca}^{2+}$ -regulated photoproteins—aequorin from *A. victoria*, obelins from *O. longissima* and *O. geniculata*, clytin from *C. gregaria*, and mitrocomin from *M. cellullaria*—as calcium indicators in a set of identical in vitro and in vivo experiments.

## Materials and methods

### Plasmid constructions and site-directed mutagenesis

For expression in cytoplasm of Chinese hamster ovary (CHO) cells, the coding sequences of the hydromedusan photoproteins were amplified by *Pfu* DNA polymerase (Sibenzyme, Russia) with specific primers (Table S1) containing *KpnI* and *XhoI* sites for cloning, and after digestion were ligated into the *KpnI/XhoI* sites of the expression vector pcDNA3.1(+) (Life Technologies). The resulting expression

plasmids were named pcDNA-OL, pcDNA-OG, pcDNA-CL3, pcDNA-MC2, and pcDNA-AV, respectively.

For expression in mitochondria of CHO cells, the coding sequence of the clytin was amplified by *Pfu* DNA polymerase (Sibenzyme, Russia) with specific primers containing *PstI* and *XhoI* site for cloning (Table S1). After digestion the clytin sequence was inserted into the *PstI/XhoI* sites of the expression vector pCMV/myc/mito (Invitrogen) by in-frame fusion to the mitochondrial signal peptide sequence. The resulting expression plasmid was named pCMVmito-CL3. Mitrocomin mutant with an improved Kozak consensus sequence was constructed using a QuikChange site-directed mutagenesis kit (Stratagene) and pET22-MC2 expression plasmid (unpublished) as a template. Forward 5'-GCTTGGTACCAT GACTATGGGCAGCAG-3' and reverse 5'-CTGCTGCCCA TAGTCATGGTACCAAGC-3' primers were designed according to the manufacturer's protocol.

All the plasmids produced were verified by sequencing.

### Photoprotein purification

For apophotoprotein production, *Escherichia coli* BL21 Codon plus (RIPL) cells (Stratagene) transformed with pET19-OG [26], pET19-OL8 [56], pET22-A7 [57], pET22-CL3 [22], or pET22-MC2 were cultivated at 37°C in vigorously shaken ampicillin-containing LB medium. Induction was initiated with 1 mM isopropyl  $\beta$ -D-thiogalactopyranoside when the culture reached an optical density at 590 nm of 0.6–0.8. After addition of isopropyl  $\beta$ -D-thiogalactopyranoside, the cultivation of cells was continued for 3 h. The *E. coli* cells were harvested by centrifugation, the pellet was resuspended in 20 mM Tris–HCl pH 7.2 (1:5, w/v), and was disrupted by sonication (20 s, six times) on ice. Then, the mixture was centrifuged, the supernatant was discarded, and all apophotoproteins were purified from a pellet as reported for recombinant wild-type obelins [26, 54, 58]. The pellet containing the inclusion bodies was sequentially washed with the following solutions to remove contaminating substances: 150 mM NaCl, 20 mM Tris–HCl pH 7.2 (once); 1 % Triton X-100, 20 mM Tris–HCl pH 7.2 (three times); and 20 mM Tris–HCl pH 7.2 (once). All the washing procedures were performed with centrifugation (16,000g, 20 min). The final pellet was resuspended in 20 mM Tris–HCl pH 7.2, containing 6 M urea, kept at 4°C overnight, and then centrifuged (16,000g, 20 min). The purification scheme to produce photoprotein of high purity included two steps. The first step was ion-exchange chromatography of supernatant on a DEAE-Sepharose Fast Flow column (Pharmacia) equilibrated with 6 M urea, 20 mM Tris–HCl pH 7.2. The apophotoprotein was eluted with a linear salt gradient (0–0.5 M sodium acetate in 6 M urea, 20 mM Tris–HCl pH 7.2). The compound corresponding to the main peak was collected, and then the protein was concentrated by using Amicon centrifugal filters

(Millipore). To fold and charge the apophotoprotein, the concentrated sample containing 6 M urea was diluted 20-fold with a solution containing 5 mM EDTA, 5 mM dithiothreitol, 20 mM Tris-HCl pH 7.2, and coelenterazine (Prolume, Pinetop, USA) (coelenterazine/apophotoprotein ratio is approximately 1.2 mol/mol) and incubated overnight at 4 °C. The coelenterazine concentration was determined using  $\varepsilon_{435\text{ nm}} = 9,800\text{ cm}^{-1}\text{ M}^{-1}$  as the absorption coefficient [1]. The charged protein was then additionally purified on a Mono Q column (GE Healthcare) equilibrated with 5 mM EDTA, 20 mM Tris-HCl pH 7.2. The photoprotein was eluted with a linear salt gradient (0–0.35 NaCl in 5 mM EDTA, 20 mM Tris-HCl pH 7.2). This chromatography step allows separation of the charged photoprotein from apoprotein that has not been charged with coelenterazine. The final photoprotein preparations were homogeneous according to sodium dodecyl sulfate–polyacrylamide gel electrophoresis analysis (Fig. S1).

#### Calcium concentration–effect curves and rapid-mixing kinetic measurements

The measurements were performed with EDTA-free solutions of photoproteins. EDTA was removed from the purified photoproteins by gel filtration on a 1.5 cm×6.5 cm D-Salt dextran desalting column (Pierce). The column was equilibrated and the photoprotein was eluted with 150 mM KCl, 5 mM piperazine-1,4-bis(2-ethanesulfonic acid) (PIPES), pH 7.0 previously passed (twice) through freshly washed beds of Chelex 100 chelating resin (Sigma) to remove trace amounts of  $\text{Ca}^{2+}$ . The fractions containing photoprotein were identified by bioluminescence assay. To avoid possible contamination with EDTA, only the first few photoprotein fractions to come off the column were used to determine  $\text{Ca}^{2+}$  concentration–effect curves and bioluminescence kinetics.

Ca-EGTA buffers (total EGTA concentration 2 mM) were used to establish  $\text{Ca}^{2+}$  concentrations below about 10  $\mu\text{M}$ , and simple dilutions of  $\text{CaCl}_2$  (in a Chelex-scrubbed solution of 150 mM KCl, 5 mM PIPES, pH 7.0) were used to establish higher  $\text{Ca}^{2+}$  concentrations. The  $\text{Ca}^{2+}$  buffers were prepared by the two-stock-solution method, and were corrected as described elsewhere [59]. According to this method, two stock solutions (2 mM EGTA pH 7.0 and 2 mM Ca-EGTA pH 7.0) are mixed in different proportions. For the  $\text{Ca}^{2+}$  concentration–effect curves, peak light intensity was measured after 10  $\mu\text{l}$  of photoprotein solution had been injected by a CR 700-20 constant-rate syringe (Hamilton, USA) into 1 ml of the test solution. Light intensity ( $L$ ) measurements were converted to units of  $L/L_{\text{int}}$  by first calculating  $L/L_{\text{max}}$  and then multiplying this by the maximum peak-to-integral ratio ( $L_{\text{max}}/L_{\text{int}}$ ) determined from kinetic measurements performed under the same conditions and with the same samples of photoproteins. The advantages of expression of light signals in  $L/L_{\text{int}}$  units were discussed elsewhere [26, 54]. All measurements were

performed at 20 °C using a luminometer equipped with a temperature-stabilized cuvette block and neutral-density filters with different transmission coefficients to fit light signals from low to saturated calcium concentrations ranging over approximately 8 log units [60].

The  $\text{Ca}^{2+}$  concentration detection limit was estimated as the  $\text{Ca}^{2+}$  concentration which will give a light signal five times the level of  $\text{Ca}^{2+}$ -independent luminescence and was calculated as the mean of the detection limits estimated from three or four  $\text{Ca}^{2+}$  concentration–effect curves for each photoprotein. The stated error is the standard deviation. The apparent dissociation constants ( $K_d$ ) were estimated from  $\text{Ca}^{2+}$  concentration–effect curves using a two-state model [61].

The light response kinetics after sudden exposure to a saturating  $\text{Ca}^{2+}$  concentration was examined with an SX20 stopped-flow machine (cell volume 20  $\mu\text{l}$ , dead-time 1.1 ms) (Applied Photophysics, UK). The temperature was controlled with a circulating water bath and was set at 20 °C. The  $\text{Ca}^{2+}$  syringe contained 40 mM  $\text{Ca}^{2+}$ , 30 mM KCl, 5 mM PIPES buffer, pH 7.0. The photoprotein was dissolved in a  $\text{Ca}^{2+}$ -free solution of the same ionic strength: 150 mM KCl, 5 mM PIPES, pH 7.0. Both syringes were prewashed with the EGTA solution and then, thoroughly, with deionized water. The solutions were mixed in equal volumes; thus, the final  $\text{Ca}^{2+}$  concentration in the reaction mixture was 20 mM. The rise rate constant was calculated by a one-exponential fit with Sigma Plot in the range from zero time to the time when the light signal reaches a maximum using the equation  $L = L_0 + a(1 - e^{-k_{\text{rise}}t})$ . The decay rate constants were calculated by two-exponential fitting. The contribution of decay rate constants  $k_1$  and  $k_2$  was estimated as the relative amplitude calculated from the fitted amplitudes  $a$  and  $b$  with their sum normalized to 1 [62]. The rise and decay rate constants were calculated as the mean of the corresponding constants determined from about ten shots, and the stated error is the standard deviation. The kinetic measurements were performed at 20 °C.

When measurements for  $\text{Ca}^{2+}$  concentration–effect curves and kinetics were to be made in solutions containing 1 mM  $\text{Mg}^{2+}$ , the photoprotein samples were pre-equilibrated for 1 h with this  $\text{Mg}^{2+}$  concentration. For these measurements, all other solutions (Ca-EGTA buffers, dilutions of  $\text{CaCl}_2$ , and  $\text{Ca}^{2+}$  solution in a syringe for rapid-mixing kinetic measurements) also contained 1 mM  $\text{Mg}^{2+}$ .

#### Transient transfection of CHO cells

For expression of different photoprotein genes, CHO cells were transfected with all pcDNA3.1(+) constructs and pCMVmito-CL3 plasmid with the use of Lipofectamine 2000 reagent (Invitrogen) in accordance with the manufacturer's protocol. The transfected cells were grown in



Dulbecco's modified Eagle's medium (DMEM)/F12 medium supplemented with 10 % fetal calf serum at 37 °C, 5 %  $\text{CO}_2$  for 24 h. Then, growth medium was removed and cells were loaded with 5  $\mu\text{M}$  coelenterazine in 130 mM NaCl, 5 mM KCl, 1 mM  $\text{MgCl}_2$ , 2 mM  $\text{CaCl}_2$ , 5 mM  $\text{NaHCO}_3$ , 20 mM *N*-(2-hydroxyethyl)piperazine-*N'*-ethanesulfonic acid (HEPES), pH 7.4 for 4 h at ambient temperature. Bioluminescence was determined with a Mithras LB 940 plate luminometer (Berthold, Germany) at 23 °C by injection of 1 % Triton X-100 in 130 mM NaCl, 5 mM KCl, 1 mM  $\text{MgCl}_2$ , 2 mM  $\text{CaCl}_2$ , 5 mM  $\text{NaHCO}_3$ , 20 mM HEPES, pH 7.4 for cell lysis and light triggering. Bioluminescence was measured by integrating the light signal for 10 s.

#### CHO cells stably expressing photoproteins

To produce stable CHO cell lines, the cells transfected with pcDNA-OL, pcDNA-OG, pcDNA-CL3, pcDNA-AV, or pCMVmito-CL3 plasmid were seeded on six-well plates and grown in the same medium with addition of Geneticin sulfate (G418) (Gibco, UK) at 1 mg/ml under the same conditions with replacement of the medium by fresh medium every 2 days. After 7–10 days of selection, CHO cells were transferred into a medium without antibiotic. To select clones with the highest bioluminescence activity, one run of limiting dilution was performed. CHO cells after G418 selection were seeded on 96-well plates (approximately 0.5 cells per well) and grown in DMEM/F12 medium supplemented with 10 % fetal calf serum at 37 °C, 5 %  $\text{CO}_2$  for up to 80–90 % confluence. Before the bioluminescence measurements, the plates with monoclonal CHO cells expressing the corresponding photoprotein were duplicated and grown for up to 90–100 % confluence. Then, the medium was removed, cells were loaded with coelenterazine, and bioluminescence in each well was measured according to the procedure described earlier. As a result, the CHO cell clones with the highest bioluminescence activity were selected. Thus, four CHO cell lines stably expressing aequorin (named CHO/pcDNA3/AV), obelins from *O. longissima* (CHO/pcDNA3/OL) and *O. geniculata* (CHO/pcDNA3/OG), and clytin (CHO/pcDNA3/CL3) in cytoplasm, and one CHO cell line stably expressing clytin (CHO/pCMVmito/CL3) in mitochondria were produced.

#### Assay of activation of endogenous $\text{P2Y}_2$ receptor in CHO cells

The CHO cell lines stably expressing each photoprotein were used in assay of activation of endogenous  $\text{P2Y}_2$  receptor by ATP. The day before the measurements, the corresponding cells were seeded on 96-well plates with DMEM/F12 medium supplemented with 10 % fetal calf serum and were grown at 37 °C with 5 %  $\text{CO}_2$  for up to 90–100 % confluence. Then, the

medium was replaced by 100  $\mu\text{l}$  of coelenterazine solution per well (5  $\mu\text{M}$  coelenterazine in 130 mM NaCl, 5 mM KCl, 1 mM  $\text{MgCl}_2$ , 2 mM  $\text{CaCl}_2$ , 5 mM  $\text{NaHCO}_3$ , 20 mM HEPES, pH 7.4) and the cells were incubated at 23 °C for 4 h. Emission from photoproteins in the cells was measured using a Mithras LB 940 plate luminometer. The ATP was injected at a given concentration to trigger an intracellular  $\text{Ca}^{2+}$  response in the cells. The measurement was started immediately. The bioluminescence was assayed by integration over a time interval of 0.05 s for 30 and 45 s for CHO cells expressing photoproteins in cytoplasm and clytin in mitochondria, respectively.

## Results and discussion

#### Calcium concentration–effect relation

Figure 1 and Table 1 summarize  $\text{Ca}^{2+}$  concentration–effect relations and some bioluminescence characteristics for the five recombinant photoproteins. Aequorin is the most sensitive to  $\text{Ca}^{2+}$  among the photoproteins tested; the  $\text{Ca}^{2+}$  concentration detection limit (i.e., when bioluminescence begins reliably to respond to a change in  $\text{Ca}^{2+}$  concentration) for aequorin is approximately 24 nM, and the apparent dissociation constant ( $K_d$ ) is 45 nM. In contrast, clytin is less sensitive to calcium since its bioluminescence starts to rise in response to a change in  $\text{Ca}^{2+}$  concentration only at 490 nM.  $K_d$  for clytin is one order of magnitude higher (Table 1). The obelins and mitrocomin also reveal approximately threefold to fivefold higher  $\text{Ca}^{2+}$  concentration detection limits than aequorin. It is noteworthy that the obelins, with a degree of identity of the amino acid sequences of 86 % [26], also differ slightly in sensitivity to calcium (Table 1).  $K_d$  for recombinant aequorin

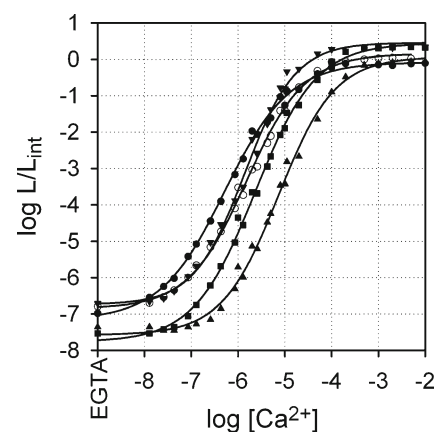


**Fig. 1**  $\text{Ca}^{2+}$  concentration–effect curves for the photoproteins aequorin (filled circles), obelins from *Obelia longissima* (inverted triangles) and *Obelia geniculata* (squares), clytin (upright triangles), and mitrocomin (open circles).  $L$  and  $L_{\text{int}}$  are the peak bioluminescence intensity for a given  $\text{Ca}^{2+}$  concentration and the total bioluminescence recorded for a saturating  $\text{Ca}^{2+}$  dose for the same sample, respectively. EGTA ethylene glycol tetraacetic acid

**Table 1** Luminescence properties of photoproteins

Photoprotein	$[Ca^{2+}]_{limit}^a$ (nM)		$K_d$ (nM)	
	Without $Mg^{2+}$	With 1 mM $Mg^{2+}$	Without $Mg^{2+}$	With 1 mM $Mg^{2+}$
Aequorin	24±2	54±2	45±5	83±5
Obelin from <i>Obelia longissima</i>	81±3	135±5	91±10	132±11
Obelin from <i>Obelia geniculata</i>	117±2	150±3	125±9	164±13
Clytin	490±20	490±10	500±35	500±45
Mitrocomin	72±3	100±2	117±14	166±17

<sup>a</sup>  $Ca^{2+}$  concentration detection limit; see the comments in “Materials and methods.”

estimated in our experiments using the two-state model is approximately threefold higher than that calculated for native aequorin ( $K_d=14$  nM [61]) but is practically equal to  $K_d$  (54 nM) determined for the other isoform of recombinant aequorin [54]. The difference in  $K_d$  values for recombinant and native aequorins may be because native aequorin was a mixture of several isoforms differing in properties [63] or because  $Ca^{2+}$  concentration–effect curves for native and recombinant aequorins were determined under slightly different conditions [61].

The very low level of light emitted by photoproteins in the absence of calcium ions (“ $Ca^{2+}$ -independent luminescence” [61]) is a result of a spontaneous decarboxylation reaction of the bound 2-hydroperoxycoelenterazine initiated by protein structural fluctuations (Fig. 1). As spontaneous photoprotein discharging within cells can decrease the amount of an active photoprotein, the  $Ca^{2+}$ -independent luminescence level may be an important factor in photoprotein selection for in vivo applications. Although all photoproteins show a low level of  $Ca^{2+}$ -free luminescence (Fig. 1), the  $Ca^{2+}$ -independent luminescence of obelin from *O. geniculata* and clytin is notably lower compared with that of other photoproteins. Luminescence of aequorin, mitrocomin, and the twoobelins reaches saturation at a  $Ca^{2+}$  concentration of approximately  $10^{-4}$ – $10^{-3}$  M, whereas that of clytin reaches saturation at a  $Ca^{2+}$  concentration above  $10^{-3}$  M (Fig. 1). As a result of this and because clytin is more insensitive to calcium, its  $Ca^{2+}$  concentration–effect curve lies to the right of those of the other photoproteins. Between  $Ca^{2+}$ -independent and saturating levels, the curves span vertical ranges of approximately 7–8 log units depending on the photoprotein. However, despite some differences, all the curves have the same maximum slope of approximately 2.5, indicating that binding of three calcium ions is necessary to trigger bioluminescence [26, 54, 61].

Another property of  $Ca^{2+}$ -regulated photoproteins that has to be taken into account is the effect of  $Mg^{2+}$  on photoprotein bioluminescence. The concentration of free  $Mg^{2+}$  in cells exceeds the  $Ca^{2+}$  concentration by several orders of magnitude [49, 50]. As competition from this cation may decrease the affinity of  $Ca^{2+}$ -binding sites of many EF-hand  $Ca^{2+}$ -binding proteins [64], this could also be the case for photoproteins owing to their belonging to the same

superfamily. Figure S2 and Table 1 summarize the effect of 1 mM  $Mg^{2+}$  on  $Ca^{2+}$  concentration–effect relations for the recombinant photoproteins. Although all the photoproteins contain three EF-hand  $Ca^{2+}$ -binding sites, revealing a high degree of amino acid sequence identity [26],  $Mg^{2+}$  noticeably affects only aequorin. The presence of 1 mM  $Mg^{2+}$  shifts the  $Ca^{2+}$  concentration–effect curve of aequorin to the right owing to a decrease of peak light intensities. However, the  $Ca^{2+}$  concentration–effect curves obtained in the absence of  $Mg^{2+}$  and in the presence of 1 mM  $Mg^{2+}$  become identical close to the saturating  $Ca^{2+}$  concentration (Fig. S2, plot A). In addition,  $Mg^{2+}$  ions also cause the  $Ca^{2+}$  concentration detection limit and  $K_d$  to increase by approximately two times (Table 1). A similar effect of  $Mg^{2+}$  on  $K_d$  was observed for the other isoform of recombinant aequorin [54]; in the presence of 1 mM  $Mg^{2+}$ ,  $K_d$  also increases approximately twofold (100 nM). The effect of  $Mg^{2+}$  ions on the  $Ca^{2+}$  concentration–effect relations of other photoproteins is less pronounced; 1 mM  $Mg^{2+}$  slightly increases the  $Ca^{2+}$  concentration detection limit and  $K_d$  for the obelins but practically does not affect those of mitrocomin and clytin (Table 1). It is noteworthy that whereas  $Ca^{2+}$ -independent luminescence of aequorin is decreased by  $Mg^{2+}$  (Fig. S2, plot A),  $Mg^{2+}$  ions increase  $Ca^{2+}$ -independent luminescence of mitrocomin (Fig. S2, plot B).

Thus, physiological concentration of  $Mg^{2+}$  removes aequorin’s advantage of higher sensitivity to  $Ca^{2+}$  relative to the other photoproteins in its use within cells.

#### Rapid-mixing stopped-flow kinetics

The rate of rise of light intensity after rapid mixing with  $Ca^{2+}$  is what limits the ability of the light signal to follow rapid changes in  $Ca^{2+}$  concentration. Hydromedusan recombinant photoproteins significantly differ from each other (Fig. 2, left panel). The rate constants calculated for the rising phase ( $k_{rise}$ ) of the light signal by fitting the experimental data of each curve to a simple exponential are summarized in Table 2. Among the photoproteins tested, obelin from *O. geniculata* shows the highest rate ( $k_{rise}=607\pm4.6$  s<sup>-1</sup>) for the rise of the luminescence signal, whereas aequorin has the lowest rate constant ( $k_{rise}=123\pm0.5$  s<sup>-1</sup>). Despite the obelins having a high degree of identity of the amino acid sequences [26],  $k_{rise}$

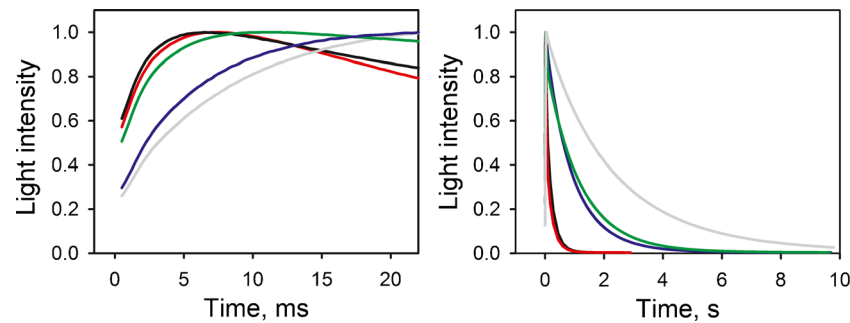


**Fig. 2** Stopped-flow records of the luminescence signal for obelins from *O. geniculata* (black) and *O. longissima* (red), clytin (green), mitrocomin (blue), and aequorin (gray). The panels on the left and right show the rising phase and full time course of the light signals, respectively. The

display begins at the time the flow was stopped, and each tracing was normalized to its own maximum to facilitate comparison of the rise time. Sampling intervals were 0.25–0.5 ms and 5–10 ms for the rising phase and the full time course, respectively

for obelin from *O. longissima* is approximately 1.2 times lower than that for obelin from *O. geniculata* (Table 2). It is noteworthy that the rate of the luminescence rise of the photoproteins, except for mitrocomin, becomes a little less after 1 week of their being in  $\text{Ca}^{2+}$ -free and EGTA-free buffer at 4 °C as compared with freshly prepared proteins (data not shown). It should also be noted that the  $k_{\text{rise}}$  values for both recombinant obelins and recombinant aequorin determined in our experiments are somewhat higher than previously reported [26, 54], which may be due to the use of different stopped-flow machines. The presence of 1 mM  $\text{Mg}^{2+}$  has a stronger effect on aequorin again. Whereas the rate of the rise of the aequorin light signal decreases almost twofold, the  $k_{\text{rise}}$  values for the other photoproteins decrease only slightly in the presence of 1 mM  $\text{Mg}^{2+}$  (Table 2, Fig. 3).

The decay of light emission is much slower compared with the rise (Fig. 2, right panel, Table 2). Whereas the decay kinetics of aequorin, mitrocomin, and clytin can be satisfactorily characterized by a single rate constant, the decay kinetics of both obelins are described by a two-exponential decay function and consequently by two rate constants—“fast” ( $k_1$ ) and “slow” ( $k_2$ ) (Table 2). The luminescence decay rates of aequorin, clytin, and mitrocomin are slow and very similar to each other; the decay constants are in the range 0.81–1.1  $\text{s}^{-1}$ . The decay kinetics of the obelins are much faster than those of

the other hydromedusan photoproteins and are very similar to each other, with only a small difference in the contribution of “fast” and “slow” rates. The presence of 1 mM  $\text{Mg}^{2+}$  reduces the luminescence decay rate of aequorin, mitrocomin, and clytin, and the influence of  $\text{Mg}^{2+}$  on the aequorin decay rate is stronger again (Table 2). The effect of magnesium on the decay kinetics of the obelins is more complicated; 1 mM  $\text{Mg}^{2+}$  decreases the rate constants of the “slow” component ( $k_2$ ) but increases the rate constants of the “fast” component ( $k_1$ ) of the decay (Table 2).

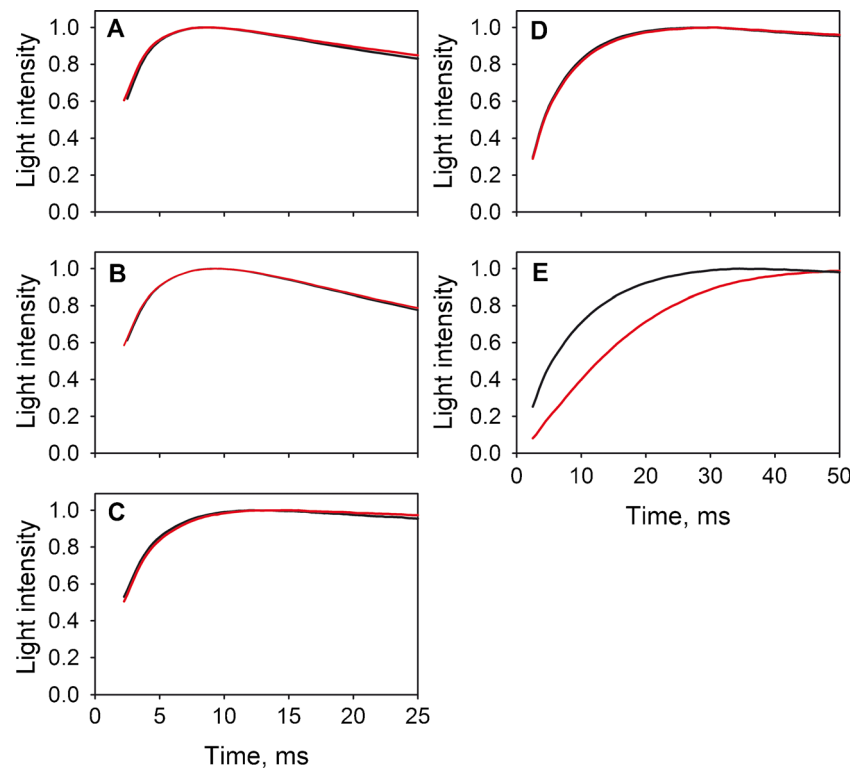
The EF-hand  $\text{Ca}^{2+}$ -binding proteins may contain two kinds of  $\text{Ca}^{2+}$ -binding EF-hands, which can be classified as  $\text{Ca}^{2+}/\text{Mg}^{2+}$ -specific and  $\text{Ca}^{2+}$ -specific types differing by their selectivity and affinity for  $\text{Ca}^{2+}$  and  $\text{Mg}^{2+}$ . Although  $\text{Ca}^{2+}$ -specific EF-hands also bind  $\text{Mg}^{2+}$ ,  $\text{Ca}^{2+}/\text{Mg}^{2+}$ -binding sites have a  $\text{Mg}^{2+}$  affinity severalfold higher [64]. Recently, with use of NMR spectroscopy it was shown that EF-hand I and EF-hand III of aequorin bind  $\text{Mg}^{2+}$  ions, and the affinity of  $\text{Ca}^{2+}$ -binding site III for  $\text{Mg}^{2+}$  is tenfold higher than that of  $\text{Ca}^{2+}$ -binding site I [65]. This result clearly evidences that  $\text{Ca}^{2+}$ -binding site III of aequorin belongs to the  $\text{Ca}^{2+}/\text{Mg}^{2+}$ -specific type and it may be a cause of the strong effect of  $\text{Mg}^{2+}$  on both the sensitivity of aequorin to  $\text{Ca}^{2+}$  and its bioluminescence kinetics. So far, there are no data available concerning specificity of  $\text{Ca}^{2+}$ -binding sites for  $\text{Mg}^{2+}$  for other

**Table 2** Rate constants for the rise and decay of bioluminescence for recombinant hydromedusan photoproteins

Photoprotein	$k_{\text{rise}}$ ( $\text{s}^{-1}$ )		$k_{\text{decay}}$ ( $\text{s}^{-1}$ )			
	Without $\text{Mg}^{2+}$	With 1 mM $\text{Mg}^{2+}$	Without $\text{Mg}^{2+}$		With 1 mM $\text{Mg}^{2+}$	
			$k_1^a$	$k_2$	$k_1^a$	$k_2$
Obelin from <i>O. geniculata</i>	607±5	594±6	40.00±0.26 (0.43)	4.80±0.01 (0.57)	47.60±0.34 (0.38)	4.50±0.01 (0.62)
Obelin from <i>O. longissima</i>	510±5	496±4	40.00±1.75 (0.66)	4.80±0.05 (0.34)	42.40±1.70 (0.63)	4.43±0.07 (0.37)
Clytin	413±3	395±5	0.88±0.01 (1)	-	0.83±0.01 (1)	-
Mitrocomin	183±2	176±1	1.10±0.01 (1)	-	1.09±0.01 (1)	-
Aequorin	123±1	66±1	0.81±0.01 (1)	-	0.71±0.01 (1)	-

<sup>a</sup> The relative contributions of individual decay constants are shown in parentheses (see “Materials and methods”)

**Fig. 3** Stopped-flow records showing the rising phase for recombinant obelins from *O. geniculata* (A) and *O. longissima* (B), recombinant clytin (C), recombinant mitrocomin (D), and recombinant aequorin (E) without  $Mg^{2+}$  (black) and with 1 mM  $Mg^{2+}$  (red). The display begins at the time the flow was stopped, and each tracing was normalized to its own maximum. The sampling interval was 0.25–0.5 ms. Before measurements, photoproteins were pre-equilibrated with 1 mM  $Mg^{2+}$  for 1 h



photoproteins, but we can reasonably assume that their  $Ca^{2+}$ -binding sites belong to  $Ca^{2+}$ -specific type on the basis of the fact that physiological concentration of  $Mg^{2+}$  has little effect on their bioluminescence.  $Mg^{2+}$  affects bioluminescence of the other photoproteins but at higher concentrations. For example, 10 mM  $Mg^{2+}$  shifts the  $Ca^{2+}$  concentration–effect curves of the obelins from *O. geniculata* and *O. longissima* to the right, decreases the level of their  $Ca^{2+}$ -independent luminescence, and slows the bioluminescence kinetics [26, 54]. Thus,  $Mg^{2+}$  comes into play only at concentrations corresponding to an affinity for  $Mg^{2+}$  (2–10 mM) determined for  $Ca^{2+}$ -binding site I of aequorin [65], thereby suggesting that the affinities of the  $Ca^{2+}$ -binding sites of the obelins are in the same range. As  $Mg^{2+}$  does not significantly affect clytin and mitrocomin bioluminescence, we may reasonably assume that the affinities of the  $Ca^{2+}$ -binding sites for  $Mg^{2+}$  for these photoproteins are very similar to those of the obelins.

#### Photoprotein-based cellular assay for endogenous $P2Y_2$ receptor in CHO cells

Since  $Ca^{2+}$ -regulated photoproteins are mainly applied to detect intracellular  $Ca^{2+}$  in mammalian cells, all recombinant wild-type photoproteins were tested for their capacity to be expressed and converted into active photoproteins in CHO cells, and in the assay of activation of endogenous cellular receptors. The ability of the different photoproteins to be expressed and converted into active photoprotein was verified using CHO cells transiently transfected with the

corresponding plasmid. For that, the day after transfection, CHO cells were incubated with coelenterazine for 4 h, and, after cell lysis with 1 % Triton X-100, bioluminescence was measured by integrating the light signals for 10 s. Whereas CHO cells expressing the recombinant aequorin, clytin, and obelins revealed good bioluminescence activities, the cells transfected with plasmid with mitrocomin showed light signals which are only a little more intense than the background signals (data not shown). The causes may be inefficient expression or conversion of apophotoprotein into active mitrocomin within cells. Low mitrocomin expression may

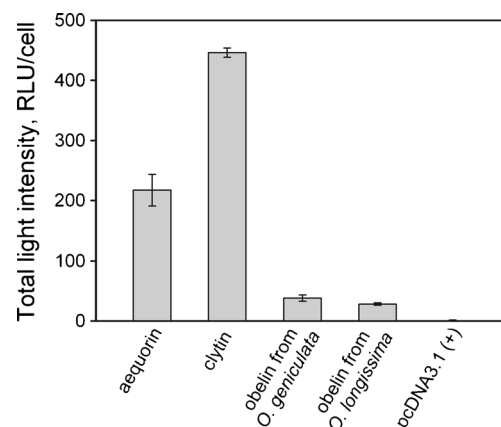


**Fig. 4** Bioluminescence activity of Chinese hamster ovary (CHO) cells stably expressing photoproteins shown as the total light signal calculated per cell. The total light intensity was measured by integration of the light signal for 10 s. Each point is the mean  $\pm$  the standard deviation (SD) of ten experiments. *RLU* relative light units



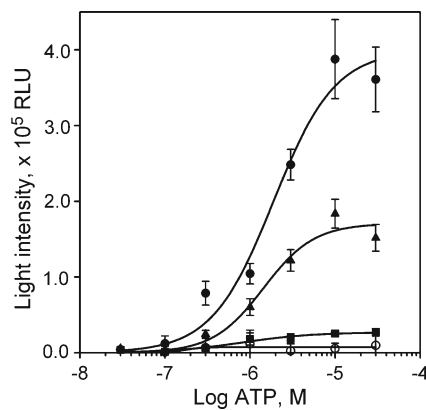


**Fig. 5** Dose-response curves for activation with ATP of endogenous  $\text{P2Y}_2$  receptor of CHO cells stably expressing aequorin (filled circles), obelins from *O. longissima* (triangles) and *O. geniculata* (squares), and clytin (open circles) in cytoplasm. The ATP concentrations are 0.03, 0.1, 0.3, 1.0, 3.0, 10.0, and 30.0  $\mu\text{M}$ . The light intensity was measured by integration of the bioluminescence signal for 30 s. Each point is the mean  $\pm$ SD of eight experiments

be caused by nonoptimal context of the AUG start codon of the mitrocomin gene, leading to its inefficient translation in mammalian cells. The sequences around the AUG start codon of most eukaryotic messenger RNAs with high translation efficiency reveal a strong compliance with the Kozak consensus sequence [66]. Both obelin genes have a strong Kozak consensus sequence—ACC ATGG—with guanine in the fourth position (numbering from the first adenine of the ATG start codon), and clytin and aequorin genes carry adenine in this position, which is also acceptable (Fig. S3). However, in the mitrocomin gene this position is occupied by thymine, resulting in a weak Kozak context. To improve the Kozak context and, consequently, to enhance the efficiency of translation initiation of the mitrocomin gene, thymine in the fourth position of the mitrocomin gene was replaced by adenine, which makes the Kozak context of the mitrocomin gene similar to the contexts of the clytin and aequorin genes, which revealed maximal bioluminescence activities in CHO cells. As

mutation did not increase the intensity of the bioluminescence signals from CHO cells, it may be concluded that, most likely, the low bioluminescence activity of CHO cells is accounted for by inefficient conversion of apo-mitrocomin into active photoprotein within cells, especially as this is consistent with the efficiency of apo-mitrocomin charging with coelenterazine in vitro. The yield of active mitrocomin obtained by standard procedures of purification and conversion of recombinant apophotoproteins produced in *E. coli* cells [26, 54, 58] is only approximately 10–20 %, whereas the yield of the other hydromedusan photoproteins is four times higher (approximately 70–80 %).

Photoprotein-based cellular assay of activation of endogenous  $\text{P2Y}_2$  purinoreceptor was conducted with CHO cells stably expressing wild-type aequorin (CHO/pcDNA3/AV), obelin from *O. longissima* (CHO/pcDNA3/OL), obelin from *O. geniculata* (CHO/pcDNA3/OG), and clytin (CHO/pcDNA3/CL3). The CHO cells stably expressing mitrocomin were not produced because their bioluminescence signals after transient transfection were close to the background level. The bioluminescence activity of stable cell lines was estimated as the total light emitted per CHO cell after lysis with 1 % Triton X-100 (Fig. 4). Despite the fact that the same procedure was applied to produce stable cell lines, the bioluminescence signals from cells expressing wild-type aequorin, clytin, and obelins differed significantly. The highest light signals were detected for cells stably expressing clytin, and exceeded twice those from cells expressing aequorin, and almost tenfold those from cells expressing the obelins (Fig. 4). We made several attempts to produce CHO cells stably expressing the obelins with bioluminescence activity per cell comparable to that for cells stably expressing aequorin and clytin. However, all our attempts failed; the bioluminescence signals from cells expressing the obelins were always approximately tenfold lower than those of cells expressing aequorin and clytin.

In CHO cells, activation of the endogenous  $\text{P2Y}_2$  purinoreceptor with ATP leads to activation of the inositol

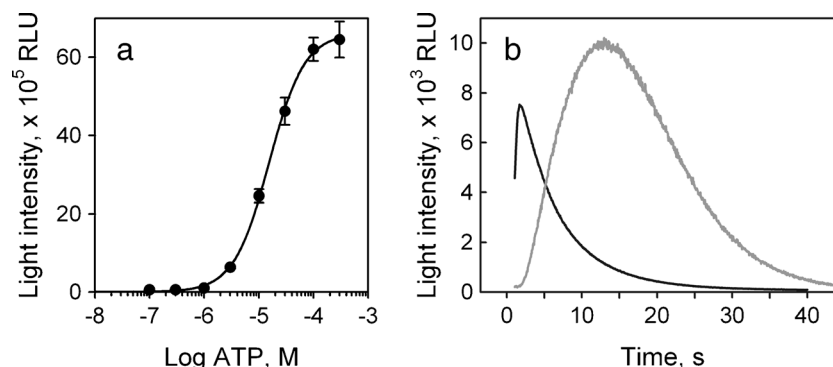


**Fig. 6** **a** Dose-response curve for activation with ATP of endogenous  $\text{P2Y}_2$  receptor of CHO cells stably expressing clytin in mitochondria. The ATP concentrations are 0.1, 0.3, 1, 3, 10, 30, 100, and 300  $\mu\text{M}$ . The light intensity was measured by integration of the bioluminescence signal for

45 s. Each point is the mean  $\pm$ SD of eight experiments. **b** Bioluminescence response kinetics of CHO cells stably expressing clytin (gray) in mitochondria and aequorin (black) in cytoplasm on adding 10  $\mu\text{M}$  ATP

1,4,5-trisphosphate signaling pathway, followed by an increase of  $\text{Ca}^{2+}$  concentration in cytoplasm. On  $\text{P2Y}_2$  receptor activation by ATP, the CHO cells stably expressing aequorin and obelin from *O. longissima* show a pronounced dose-dependent response (Fig. 5). The median effective concentrations for  $\text{P2Y}_2$  receptor activation determined with cell lines expressing aequorin and obelin were estimated as 2.8  $\mu\text{M}$  and 2.2  $\mu\text{M}$ , respectively, which match well those earlier reported [57, 67]. Despite the fact that cells stably expressing clytin revealed the highest bioluminescence activity, and the bioluminescence signals from cells stably expressing obelin from *O. geniculata* were similar to those of cells expressing obelin from *O. longissima* (Fig. 4), no dependence of activation on ATP for these stable cell lines was revealed (Fig. 5). This is most probably caused by a higher  $\text{Ca}^{2+}$  concentration detection limit for obelin from *O. geniculata* and clytin as compared with that for obelin from *O. longissima* and aequorin (Table 1). This supposition was verified with a stable CHO cell line (CHO/pCMVmito/CL3) expressing clytin containing signal peptide for direction of photoprotein into mitochondria, which have a very large capacity to accumulate  $\text{Ca}^{2+}$  during cell stimulation. These CHO cells revealed a pronounced dose-dependent response of activation of  $\text{P2Y}_2$  receptor by ATP (Fig. 6a), with a median effective concentration of 15.5  $\mu\text{M}$ , thereby indicating the correctness of our supposition. However, the bioluminescence response of cells expressing clytin in mitochondria on addition of ATP was delayed and was significantly slower than that of CHO cells expressing aequorin in cytoplasm (Fig. 6b).

## Conclusion

In summary, in this study we have reported for the first time the results of comparative characterization of five wild-type hydromedusan recombinant photoproteins—aequorin from *A. victoria*, obelins from *O. geniculata* and *O. longissima*, nitrocomin from *M. cellularia*, and clytin from *C. gregaria*—in terms of their application as intracellular calcium indicators. In a set of identical in vitro and in vivo experiments, we showed that despite a high degree of identity of the amino acid sequences [9] and spatial structures [11–13], and, apparently, a common mechanism for the bioluminescence reaction [68], these photoproteins differ in properties ( $\text{Ca}^{2+}$  concentration detection limits, sensitivities of bioluminescence to  $\text{Mg}^{2+}$ , and rates of the rise of the luminescence signal on a sudden change of  $\text{Ca}^{2+}$  concentration) which are important for measurement of intracellular  $\text{Ca}^{2+}$  concentration. Although much is known about the bioluminescence of  $\text{Ca}^{2+}$ -regulated photoproteins, the molecular mechanisms underlying their different properties are still not clear.

On the basis of our studies, we also suggest that wild-type aequorin is the best photoprotein to keep track of intracellular

$\text{Ca}^{2+}$  transients in cytoplasm of mammalian cells. However, its main shortcoming is the sensitivity of bioluminescence to  $\text{Mg}^{2+}$ , which must be taken into account in quantitative conversion of light signals into  $\text{Ca}^{2+}$  concentration. The obelin from *O. longissima* can also be used to monitor intracellular  $\text{Ca}^{2+}$  concentration dynamics in cytoplasm, although it provides lower light signals than aequorin in response to a change in  $\text{Ca}^{2+}$  concentration, at least on activation of  $\text{P2Y}_2$  receptor in CHO cells. However, its unquestionable advantage is insensitivity to  $\text{Mg}^{2+}$ , which makes quantitative determination of intracellular  $\text{Ca}^{2+}$  concentration easier. As clytin and obelin from *O. geniculata* have higher  $\text{Ca}^{2+}$  concentration detection limits, these photoproteins may be applied, probably without any modification, to monitor  $\text{Ca}^{2+}$  concentration changes in cell compartments with high  $\text{Ca}^{2+}$  concentration, such as mitochondria, the nucleus, the plasma membrane, peroxisomes, or Golgi apparatus. Moreover, bioluminescence of these photoproteins is also insensitive to  $\text{Mg}^{2+}$  ions. Thus, a suitable photoprotein depending on the task to be addressed can be selected among available hydromedusan recombinant wild-type photoproteins.

**Acknowledgments** This work was supported by RFBR grant 12-04-00131, by the programs of the Government of the Russian Federation “Measures to Attract Leading Scientists to Russian Educational Institutions” (grant 11.G34.31.0058) and “Molecular and Cellular Biology” of the Russian Academy of Sciences, and the grant from the President of the Russian Federation “Leading Science School” (3951.2012.4).

## References

1. Shimomura O (2006) Bioluminescence: chemical principles and methods. World Scientific, Singapore
2. Shimomura O, Johnson FH (1966) In: Johnson FH, Haneda Y (eds) Bioluminescence in progress. Princeton University Press, Princeton
3. Shimomura O, Johnson FH (1968) Chaetopterus photoprotein: crystallization and cofactor requirements for bioluminescence. Science 159:1239–1240
4. Müller T, Campbell AK (1990) The chromophore of pholasin: a highly luminescent protein. J Biolumin Chemilumin 5:25–30
5. Dunstan SL, Sala-Newby GB, Fajardo AB, Taylor KM, Campbell AK (2000) Cloning and expression of the bioluminescent photoprotein pholasin from the bivalve mollusc *Pholas dactylus*. J Biol Chem 275:9403–9409
6. Fujii T, Ahn JY, Kuse M, Mori H, Matsuda T, Isobe M (2002) A novel photoprotein from oceanic squid (*Symplectoteuthis oualaniensis*) with sequence similarity to mammalian carbon-nitrogen hydrolase domains. Biochem Biophys Res Commun 293: 874–879
7. Morin JG (1974) In: Muscatine L, Lenhoff HM (eds) Coelenterate biology: reviews and new perspectives. Academic, New York
8. Shimomura O, Johnson FH, Saiga Y (1962) Extraction, purification and properties of aequorin, a bioluminescent protein from the luminous hydromedusan, *Aequorea*. J Cell Comp Physiol 59:223–239
9. Vysotski ES, Markova SV, Frank LA (2006) Calcium-regulated photoproteins of marine coelenterates. Mol Biol 40:355–367

10. Shimomura O, Johnson FH (1978) Peroxidized coelenterazine, the active group in the photoprotein aequorin. *Proc Natl Acad Sci U S A* 75:2611–2615
11. Head JF, Inouye S, Teranishi K, Shimomura O (2000) The crystal structure of the photoprotein aequorin at 2.3 Å resolution. *Nature* 405:372–376
12. Liu ZJ, Vysotski ES, Deng L, Lee J, Rose J, Wang BC (2003) Atomic resolution structure of obelin: soaking with calcium enhances electron density of the second oxygen atom substituted at the C2-position of coelenterazine. *Biochem Biophys Res Commun* 311:433–439
13. Titushin MS, Feng Y, Stepanyuk GA, Li Y, Markova SV, Golz S, Wang BC, Lee J, Wang J, Vysotski ES, Liu ZJ (2010) NMR-derived topology of a GFP-photoprotein energy transfer complex. *J Biol Chem* 285:40891–40900
14. Shimomura O, Johnson FH (1972) Structure of the light-emitting moiety of aequorin. *Biochemistry* 11:1602–1608
15. Cormier MJ, Hori K, Karkhanis YD, Anderson JM, Wampler JM, Morin JG, Hastings JW (1973) Evidence for similar biochemical requirements for bioluminescence among the coelenterate. *J Cell Physiol* 81:291–297
16. Vysotski ES, Lee J (2004) Ca<sup>2+</sup>-regulated photoproteins: structural insight into the bioluminescence mechanism. *Acc Chem Res* 37:405–415
17. Prasher D, McCann RO, Cormier MJ (1985) Cloning and expression of cDNA coding for aequorin, a bioluminescent calcium-binding protein. *Biochem Biophys Res Commun* 126:1259–1268
18. Inouye S, Noguchi M, Sakaki Y, Takagi Y, Miyata T, Iwanaga S, Tsuji FI (1985) Cloning and sequence analysis of cDNA for the luminescent protein aequorin. *Proc Natl Acad Sci U S A* 82:3154–3158
19. Prasher DC, McCann RO, Longiaru M, Cormier MJ (1987) Sequence comparisons of complementary DNAs encoding aequorin isotypes. *Biochemistry* 26:1326–1332
20. Inouye S, Tsuji FI (1993) Cloning and sequence analysis of cDNA for the Ca<sup>2+</sup>-activated photoprotein, clytin. *FEBS Lett* 315:343–346
21. Inouye S (2008) Cloning, expression, purification and characterization of an isotype of clytin, a calcium-binding photoprotein from the luminous hydromedusa *Clytia gregarium*. *J Biochem* 143:711–717
22. Markova SV, Burakova LP, Frank LA, Golz S, Korostileva KA, Vysotski ES (2010) Green-fluorescent protein from the bioluminescent jellyfish *Clytia gregaria*: cDNA cloning, expression, and characterization of novel recombinant protein. *Photochem Photobiol Sci* 9:757–765
23. Fagan TF, Ohmiya Y, Blinks JR, Inouye S, Tsuji FI (1993) Cloning, expression and sequence analysis of cDNA for the Ca<sup>2+</sup>-binding photoprotein, mitrocomin. *FEBS Lett* 333:301–305
24. Illarionov BA, Markova SV, Bondar VS, Vysotski ES, Gitelson JI (1992) Cloning and expression of cDNA for the Ca<sup>2+</sup>-activated photoprotein obelin from the hydroid polyp *Obelia longissima*. *Dokl Akad Nauk* 326:911–913
25. Illarionov BA, Bondar VS, Illarionova VA, Vysotski ES (1995) Sequence of the cDNA encoding the Ca<sup>2+</sup>-activated photoprotein obelin from the hydroid polyp *Obelia longissima*. *Gene* 153:273–274
26. Markova SV, Vysotski ES, Blinks JR, Burakova LP, Wang B-C, Lee J (2002) Obelin from the bioluminescent marine hydroid *Obelia geniculata*: cloning, expression, and comparison of some properties with those of the other Ca<sup>2+</sup>-regulated photoproteins. *Biochemistry* 41:2227–2236
27. Markova SV, Burakova LP, Golz S, Malikova NP, Frank LA, Vysotski ES (2012) The light-sensitive photoprotein berovin from the bioluminescent ctenophore *Beroë abyssicola*: a novel type of Ca<sup>2+</sup>-regulated photoprotein. *FEBS J* 279:856–870
28. Aghamaali MR, Jafarian V, Sariri R, Molakarimi M, Rasti B, Taghdir M, Sajedi RH, Hosseinkhani S (2011) Cloning, sequencing, expression and structural investigation of mnemiopsin from *Mnemiopsis leidyi*: an attempt toward understanding Ca<sup>2+</sup>-regulated photoproteins. *Protein J* 30:566–574
29. Schnitzler CE, Pang K, Powers ML, Reitzel AM, Ryan JF, Simmons D, Tada T, Park M, Gupta J, Brooks SY, Blakesley RW, Yokoyama S, Haddock SH, Martindale MQ, Baxeavanis AD (2012) Genomic organization, evolution, and expression of photoprotein and opsin genes in *Mnemiopsis leidyi*: a new view of ctenophore photocytes. *BMC Biol* 10:107
30. Powers ML, McDermott AG, Shaner NC, Haddock SH (2013) Expression and characterization of the calcium-activated photoprotein from the ctenophore *Bathocyroe fosteri*: insights into light-sensitive photoproteins. *Biochem Biophys Res Commun* 431:360–366
31. Stepanyuk GA, Liu ZJ, Burakova LP, Lee J, Rose J, Vysotski ES, Wang BC (2013) Spatial structure of the novel light-sensitive photoprotein berovin from the ctenophore *Beroë abyssicola* in the Ca<sup>2+</sup>-loaded apoprotein conformation state. *Biochim Biophys Acta* 1834:2139–2146
32. Shimomura O, Johnson FH (1975) Regeneration of the photoprotein aequorin. *Nature* 256:236–238
33. Ridgway EB, Ashley CC (1967) Calcium transients in single muscle fibers. *Biochem Biophys Res Commun* 29:229–234
34. Tsien RY (1983) Intracellular measurements of ion activities. *Annu Rev Biophys Bioeng* 12:91–116
35. Bruton JD, Cheng AJ, Westerblad H (2012) Methods to detect Ca<sup>2+</sup> in living cells. *Adv Exp Med Biol* 740:27–43
36. Paredes RM, Etzler JC, Watts LT, Zheng W, Lechleiter JD (2008) Chemical calcium indicators. *Methods* 46:143–151
37. Whitaker M (2010) Genetically encoded probes for measurement of intracellular calcium. *Methods Cell Biol* 99:153–182
38. Bonora M, Giorgi C, Bononi A, Marchi S, Patergnani S, Rimessi A, Rizzuto R, Pinton P (2013) Subcellular calcium measurements in mammalian cells using jellyfish photoprotein aequorin-based probes. *Nat Protoc* 8:2105–2118
39. Ottolini D, Cali T, Brini M (2013) Measurements of Ca<sup>2+</sup> concentration with recombinant targeted luminescent probes. *Methods Mol Biol* 937:273–291
40. Rutter GA, Burnett P, Rizzuto R, Brini M, Murgia M, Pozzan T, Tavaré JM, Denton RM (1996) Subcellular imaging of intramitochondrial Ca<sup>2+</sup> with recombinant targeted aequorin: significance for the regulation of pyruvate dehydrogenase activity. *Proc Natl Acad Sci U S A* 93:5489–5494
41. Baubet V, Le Mouëllic H, Campbell AK, Lucas-Meunier E, Fossier P, Brulet P (2000) Chimeric green fluorescent protein-aequorin as bioluminescent Ca<sup>2+</sup> reporters at the single-cell level. *Proc Natl Acad Sci U S A* 97:7260–7265
42. Kendall JM, Sala-Newby G, Ghalaut V, Dormer RL, Campbell AK (1992) Engineering the Ca<sup>2+</sup>-activated photoprotein aequorin with reduced affinity for calcium. *Biochem Biophys Res Commun* 187:1091–1097
43. Tricoire L, Tsuzuki K, Courjean O, Gibelin N, Bourout G, Rossier J, Lambalez B (2006) Calcium dependence of aequorin bioluminescence dissected by random mutagenesis. *Proc Natl Acad Sci U S A* 103:9500–9505
44. de la Fuente S, Fonteriz RI, de la Cruz PJ, Montero M, Alvarez J (2012) Mitochondrial free [Ca<sup>2+</sup>] dynamics measured with a novel low-Ca<sup>2+</sup> affinity aequorin probe. *Biochem J* 445:371–376
45. Shimomura O, Musicki B, Kishi Y, Inouye S (1993) Light-emitting properties of recombinant semi-synthetic aequorins and recombinant fluorescein-conjugated aequorin for measuring cellular calcium. *Cell Calcium* 14(5):373–378
46. Inouye S, Imori R, Sahara Y, Hisada S, Hosoya T (2010) Application of new semi-synthetic aequorins with long half-decay time of luminescence to G-protein-coupled receptor assay. *Anal Biochem* 407:247–252
47. de la Fuente S, Fonteriz RI, Montero M, Alvarez J (2013) Ca<sup>2+</sup> homeostasis in the endoplasmic reticulum measured with a new low-Ca<sup>2+</sup>-affinity targeted aequorin. *Cell Calcium* 54:37–45

48. Takahashi A, Camacho P, Lechleiter JD, Herman B (1999) Measurement of intracellular calcium. *Physiol Rev* 79:1089–1125
49. White RE, Hartzell HC (1989) Magnesium ions in cardiac function. Regulator of ion channels and second messengers. *Biochem Pharmacol* 38:859–867
50. Romani AM (2011) Cellular magnesium homeostasis. *Arch Biochem Biophys* 512:1–23
51. Prendergast FG (1982) The use of photoproteins in the detection and quantitation of  $\text{Ca}^{2+}$  in biological systems. *Trends Anal Chem* 1:378–383
52. Blinks JR (1990) Use of photoproteins as intracellular calcium indicators. *Environ Health Perspect* 84:75–81
53. Stephenson DG, Sutherland PJ (1981) Studies on the luminescent response of the  $\text{Ca}^{2+}$ -activated photoprotein, obelin. *Biochim Biophys Acta* 678:65–75
54. Illarionov BA, Frank LA, Illarionova VA, Bondar VS, Vysotski ES, Blinks JR (2000) Recombinant obelin: cloning and expression of cDNA, purification and characterization as a calcium indicator. *Methods Enzymol* 305:223–249
55. Shimomura O, Shimomura A (1985) Halistaurin, phialidin and modified forms of aequorin as  $\text{Ca}^{2+}$  indicator in biological systems. *Biochem J* 228:745–749
56. Markova SV, Vysotski ES, Lee J (2001) In: Case JF, Herring PJ, Robison BH, Haddock SHD, Kricka LJ, Stanley PE (eds) *Bioluminescence & chemiluminescence 2000*. World Scientific Publishing, Singapore
57. Stepanyuk GA, Golz S, Markova SV, Frank LA, Lee J, Vysotski ES (2005) Interchange of aequorin and obelin bioluminescence color is determined by substitution of one active site residue of each photoprotein. *FEBS Lett* 579:1008–1014
58. Vysotski ES, Liu ZJ, Rose J, Wang BC, Lee J (2001) Preparation and X-ray crystallographic analysis of recombinant obelin crystals diffracting to beyond 1.1 Å. *Acta Crystallogr D* 57:1919–1921
59. Klabusay M, Blinks JR (1996) Some commonly overlooked properties of calcium buffer systems: A simple method for detecting and correcting stoichiometric imbalance in CaEGTA stock solutions. *Cell Calcium* 20:227–234
60. Blinks JR (1989) Use of calcium-regulated photoproteins as intracellular  $\text{Ca}^{2+}$  indicators. *Methods Enzymol* 172:164–203
61. Allen DG, Blinks JR, Prendergast FG (1977) Aequorin luminescence: relation of light emission to calcium concentration – a calcium-independent component. *Science* 195:996–999
62. Ereemeeva EV, Markova SV, Frank LA, Visser AJ, van Berkel WJ, Vysotski ES (2013) Bioluminescent and spectroscopic properties of His-Trp-Tyr triad mutants of obelin and aequorin. *Photochem Photobiol Sci* 12:1016–1024
63. Shimomura O (1986) Isolation and properties of various molecular forms of aequorin. *Biochem J* 234:271–277
64. Gifford JL, Walsh MP, Vogel HJ (2007) Structures and metal-ion-binding properties of the  $\text{Ca}^{2+}$ -binding helix-loop-helix EF-hand motifs. *Biochem J* 405:199–221
65. Ohashi W, Inouye S, Yamazaki T, Hirota H (2005) NMR analysis of the  $\text{Mg}^{2+}$ -binding properties of aequorin, a  $\text{Ca}^{2+}$ -binding photoprotein. *J Biochem* 138:613–620
66. Kozak M (1990) Downstream secondary structure facilitates recognition of initiator codons by eukaryotic ribosomes. *Proc Natl Acad Sci U S A* 87:8301–8305
67. Gealageas R, Malikova NP, Picaud S, Borgdorff AJ, Burakova LP, Brûlet P, Vysotski ES, Dodd RH (2014) Bioluminescent properties of obelin and aequorin with novel coelenterazine analogues. *Anal Bioanal Chem* 406:2695–2707
68. Natashin PV, Ding W, Ereemeeva EV, Markova SV, Lee J, Vysotski ES, Liu ZJ (2014) Structures of the  $\text{Ca}^{2+}$ -regulated photoprotein obelin Y138F mutant before and after bioluminescence support the catalytic function of a water molecule in the reaction. *Acta Crystallogr D* 70:720–732